Comparison of ultrafast carrier thermalization in $Ga_xIn_{1-x}As$ and Ge quantum wells

C. Lange,[1,*] N. S. Köster,[1] S. Chatterjee,[1] H. Sigg,[2] D. Chrastina,[3] G. Isella,[3] H. von Känel,[3] B. Kunert,[1] and W. Stolz[1]
[1]*Faculty of Physics and Material Sciences Center, Philipps-Universität Marburg, Renthof 5, D-35032 Marburg, Germany*
[2]*Laboratory for Micro and Nanotechnology, Paul Scherrer Institut, CH-5232 Villigen PSI, Switzerland*
[3]*Dipartimento di Fisica del Politecnico di Milano, CNISM and L-NESS, Polo di Como, via Anzani 42, I-22100 Como, Italy*
(Received 24 June 2009; revised manuscript received 5 January 2010; published 26 January 2010)

The thermalization of photoexcited carriers is investigated using femtosecond pump-probe spectroscopy in both (GaIn)As and Ge quantum wells. In both materials a nonthermal electron distribution is observed. The continuous relaxation from the point of injection toward the ground state and the thermalization of the carrier distribution are monitored on a time scale of up to 500 fs at room temperature. Carriers in (GaIn)As thermalize within 300 fs when injected with an excess energy of 250 meV. Separate carrier distributions for the heavy-hole and light-hole systems are found since the angular momentum transfer required for a transition is slow. Thermalization in Ge is found to be slightly slower in comparison due to the lack of Fröhlich interaction.

DOI: 10.1103/PhysRevB.81.045320 PACS number(s): 78.47.jh, 78.40.Fy

When a laser pulse propagates through a piece of matter, its electric field initially couples to the macroscopic polarization inside the medium according to Maxwell's equations. Polarization is then converted into population according to the semiconductor Bloch equations.[1] The carriers subsequently thermalize; i.e., they are redistributed in k space mostly by Coulomb interaction. Eventually, they can be described by a Fermi distribution.[1] In parallel, the carrier system cools down toward the lattice temperature under emission of phonons.[2] This thermalization and relaxation behavior has been investigated using various experimental methods such as pump probe,[3] spectral hole burning,[4] and luminescence,[5,6] only to name a few. However, these processes have not yet been monitored over a broad spectral range, observing thermalization from the point of injection at high excess energies down to the minima of the bands.

Here, we present experimental results for quantum well (QW) samples of the III-V compound semiconductor (GaIn)As as well as for Ge, which has recently regained attention in the photonics community.[7–9] A rigorous analysis of the spectral line shape as a function of time allows for separating shifts of the oscillators from bleaching by population. In this way the scattering times may be obtained correctly. Also, the thermalization behavior is tracked accurately and nonthermal carrier distributions are observed.

We use a tunable, relatively narrow-band transform-limited 80 fs pump pulse to excite carriers and a spectrally broad white-light supercontinuum as probe. The pump pulse is retrieved from an optical parametric amplifier (OPA) while the white light is generated in a sapphire crystal; both are driven by a 1 kHz Ti:Sapphire amplifier with 100 fs pulse duration. The white light which is intrinsically chirped in the process of generation is further broadened in time by the optics used in the experiment. In order to analyze short scattering times over a broad spectral range at once, it is crucially important to correct for this effect. We therefore employ a numerical chirp correction of the experimental data. The time zero for each energy is determined by taking into account coherent oscillations[10] from the experimental data itself. In addition, the white light is correlated with a short, transform-limited pulse in a separate experiment which confirms the position of the time zero. This approach enables the detection of the optical absorption with both high temporal and high spectral resolution and thus, the complete kinetics of the carriers are monitored.[11,12]

First, (GaIn)As QWs are studied as an example for a well-characterized III-V compound semiconductor. The sample is grown using metal-organic vapor-phase epitaxy and contains nine $(Ga_{0.67}In_{0.33})As$ QWs of 7.5 nm thickness each. The barriers consist of 104 nm $Ga(P_{0.03}As_{0.97})$ sandwiched between 10 nm GaAs. Thicknesses and compositions are designed to achieve strain compensation. Three layers, 75 nm $(Al_{0.85}Ga_{0.15})As$, 20 nm GaAs, and 200 nm $(Al_{0.85}Ga_{0.15})As$, acting as etch stop are grown between the QW stack and the semi-insulating GaAs substrate. The sample is attached to a high-purity polished sapphire substrate of 0.5 mm thickness using UV-cured polymer glue. The substrate and etch stop are subsequently removed by wet chemical etching to eliminate any spurious response from the substrate.

The differential absorption $\Delta\alpha L$, i.e., the difference in absorption of the sample in equilibrium and under excitation conditions is shown in Fig. 1 for a temperature of (a) 293 and (b) 10 K as a false-color plot. In particular, a negative value of $\Delta\alpha L$ (reddish) means a decrease in absorption and a positive value of $\Delta\alpha L$ (bluish) corresponds to an increase. Any impression of skewed streaks in the spectrum results from the numerical correction of the time zero. The pump was centered in the continuum of transition from the second heavy hole state to the second electron state (hh2-c2) at 1.3 and 1.42 eV for 293 and 10 K, respectively. A photon density of 5×10^{14} cm^{-2} was used in both cases, in combination ensuring comparable excitation conditions, i.e., similar magnitude of absorption and thus similar carrier densities. In (a), the gray-shaded area indicates the pump spectrum.

The three resonances, which are best seen in the low-temperature differential absorption spectrum, correspond to transitions from the first heavy hole (hh1) to the first electron state (c1), the first light hole (lh1) to the c1 state, and from the second heavy hole (hh2) to the second electron state (c2). The linear absorption spectrum is shown for reference as a solid black line with these transitions labeled accordingly.

Rabi flops[13] of the coherent polarization are observed around the energy of injection near time zero in (a), as can be seen by the modulated absorption intensity at this transition, and in the continuum above in energy. The polarization in GaAs-based systems dephases on a time scale which is com-

 ©2010 The American Physical Society

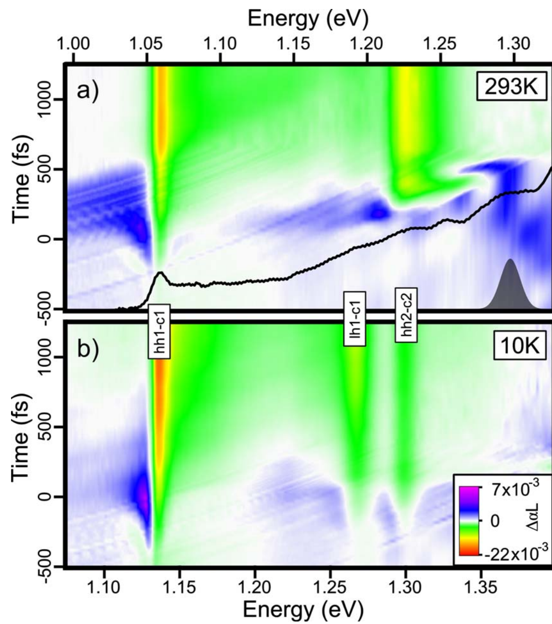

FIG. 1. (Color online). Differential absorption spectrum of the (GaIn)As quantum well sample shown in false color for (a) 293 and (b) 10 K. The sample was in both cases excited by 80 fs pulses centered in the continuum of the hh2-c2 transition. In (a), the linear absorption spectrum is shown for reference as solid black line. The three fundamental transitions can be best seen in the low-temperature differential absorption spectrum (see text).

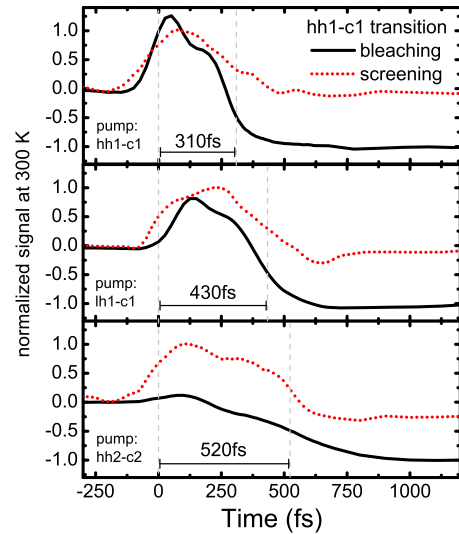

FIG. 2. (Color online). Shift and bleaching signals of the hh1-c1 transition at 293 K for varying carrier injection excess energy. Ultrafast charge screening and the ac Stark effect lead to a quasi-instantaneous shift of the resonance as the sample is excited. The population transfer from the point of injection downwards to the hh1 and c1 states at the respective band edges is delayed by 310, 430, and 520 fs for an excess energy of 90, 120, and 210 meV, respectively.

parable to the duration of our pulse. At the hh2-c2 transition, the absorption is thus bleached shortly after excitation due to strong population by the pump pulse. The hh1-c1 resonance is not bleached immediately but rather shifts toward lower energies quasi-instantaneously, as indicated by the bluish color at the low-energy side of the transition. At this time, the shift is caused by the ac Stark effect[13] which follows the exciting pulse instantaneously. An additional contribution to the shift results from screening effects[13] and band gap renormalization[13] which set in with the presence of carriers in the system at higher energies. Subsequently, carriers scatter down in energy from the point of injection and populate the states lower in energy. It is already evident from the false-color plots that the hh1-c1 resonance is bleached faster than the lh1-c1 resonance, although the latter is much closer in energy to the point of injection. This delayed population transfer is attributed to the change in angular momentum which is required when transferring holes from the hh2 state to the lh1 state. In the case of cooling, i.e., electron-phonon interaction, the angular momentum has to be provided by the phonon. The hh-lh scattering efficiencies are found to be about two orders of magnitude smaller than those between the hole bands with the same angular momentum.[14] More recently, it was shown that this angular momentum transfer is inherently inefficient, thus slowing down the intrasubband charge transfer.[15] The effect can be best observed for the 10 K measurement.

In order to analytically distinguish between bleaching and shift/broadening, a line-shape analysis is performed around the hh1-c1 transition for the two temperatures. The differential absorption is integrated in energy around this resonance. The resulting transient signal is associated with the bleaching of the resonance since it is a measure of the decrease in oscillator strength which manifests in a net loss of absorption. Any pure shift or broadening of the resonance does not yield any net contribution to the integral. Likewise, the shift signal is determined by unilaterally integrating from the center of the resonance to the high-energy side. Both signals are normalized to ease the comparison, i.e., the bleaching signal is normalized to its (negative) quasisteady-state value at >2 ps and the shift signal is normalized to the maximum value attained near time zero. In Fig. 2, the result is plotted for a temperature of 293 K and varying carrier injection energies, corresponding to the (a) hh1-c1 continuum, (b) the lh1-c1 transition, and (c) the hh2-c2 transition. The shift sets in quasi-instantaneously with the exciting pulse for all excitation energies and decays within the first 500 fs. The bleaching of the resonance is delayed by 310, 430, and 520 fs for an excess energy of 90, 120, and 210 meV, respectively. These values are linearly correlated, yielding a time offset of about 150 fs which is attributed to dephasing.

The dynamics at 10 K are plotted in Fig. 3. In order to facilitate a comparison with the measurements at 293 K, the injection is performed analogously, i.e., with respective excess energies of 80, 130, and 280 meV. At low temperatures, phonon absorption is distinctly reduced which results in a reduced efficiency of carrier cooling. The absorption at the hh1-c1 transition is now bleached significantly slower and correspondingly, the carrier-mediated shifts display slower dynamics. A relaxation time of 470 and 500 fs is determined for carrier injection in the continuum of the hh1-c1 transition and the lh1-c1 transition, respectively. For an excitation with large excess energy in the continuum of the hh2-c2 transition, intersubband scattering is required, yielding a relaxation

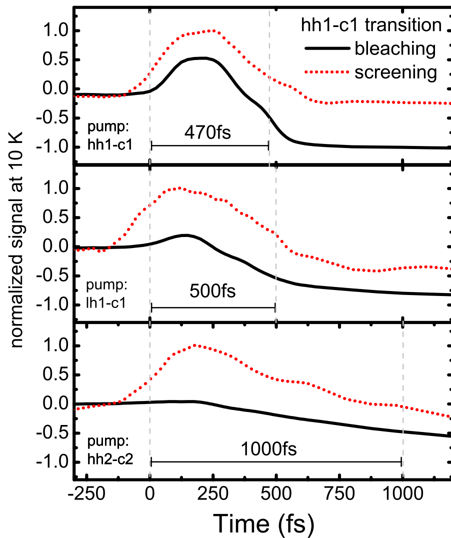

FIG. 3. (Color online). Shift and bleaching signals of the hh1-c1 transition at 10 K for varying carrier injection excess energy. The population transfer is significantly slower than at 293 K and takes 470, 500, and 1000 fs for an excess energy of 80, 130 and 280 meV, respectively.

time of 1 ps. Here, a dephasing time of 200 fs is obtained.

In Fig. 4, the bleaching signal of all transitions is plotted for excitation above the hh2-c2 transition at 293 K. The carriers relax toward the respective band edges, thereby populating the intermediate states. The hh2-c2 transition is bleached first, with the bleaching signal again exhibiting Rabi flops (dotted line). The bleaching of the hh1-c1 transition follows with a delay of 200 fs (solid line). It features a smaller slope due to the multitude of possible carrier scattering pathways from the point of injection to the hh1 and c1 states which broaden the signal in time. After another 100 fs, the bleaching of the lh1-c1 transition is observed. This again demonstrates that scattering from the hh2 into the hh1 state is faster than intersubband hole scattering from the hh2 into the lh1 state due to the required change in angular momentum as discussed above. One may consider the resulting carrier distribution either as a nonthermal distribution or as a

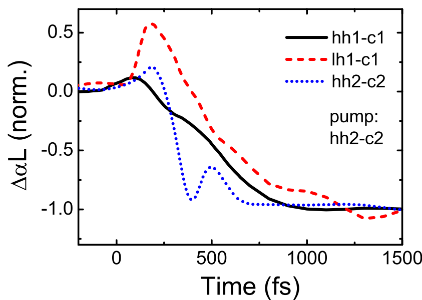

FIG. 4. (Color online). Bleaching signal at the three fundamental transitions of the GaInAs QW excited in the continuum of the hh2-c2 resonance. Rabi flops of the polarization at the hh2-c2 transition are observed. The carriers relax in energy toward the band edges and subsequently populate the states in between. This leads to bleaching at the hh1-c1 transition after 200 fs and, with a delay of 300 fs, the lh1-c1 transition.

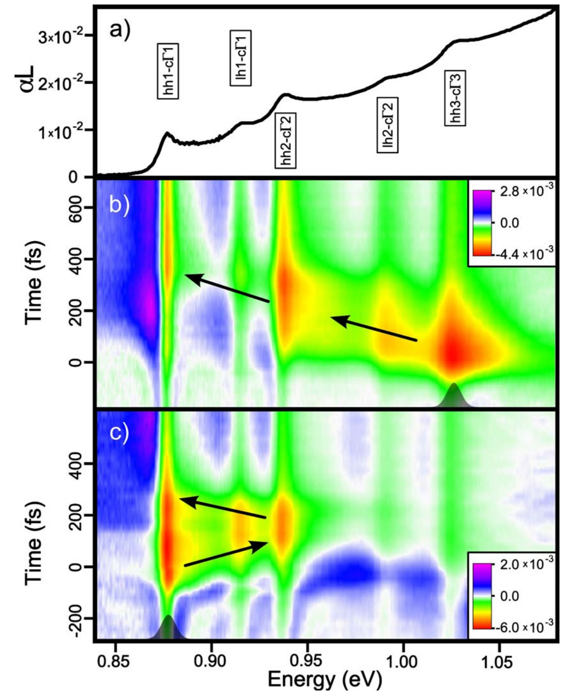

FIG. 5. (Color online) (a) Linear absorption spectrum of the Ge quantum well sample. Differential absorption spectra on a false-color scale for excitation at the (b) hh3-cΓ3 and at the (c) hh1-cΓ1 transition. The black arrows follow the relaxation.

superposition of two thermally distributed and mostly decoupled subsystems of different angular momentum, each with a different temperature. Inside each of these system, a rapid carrier cooling and redistribution drives the system toward thermal equilibrium on time scales longer than the intersubband scattering time.

Germanium QWs are studied as a second example. In germanium, the conduction band minimum is situated at the L point of the Brillouin zone. For clarity, the states around the local minimum at the Γ point are therefore referred to as cΓx. The data are taken on a heterostructure containing 50 Ge QWs grown by low-energy plasma-enhanced chemical vapor deposition.[16] A graded $Si_{1-x}Ge_x$ buffer of varying germanium concentration is grown on a Si(001) substrate. The germanium fraction is continuously increased from $x=0$ to 0.9. A concentration gradient of 7% μm^{-1} is used resulting in a total buffer thickness of 13 μm. Next, a 2 μm layer of $Si_{0.1}Ge_{0.9}$ is grown to isolate the QW stack from the strain fields of the dislocations in the graded buffer. The QW stack consists of 14.3 nm strained QWs sandwiched in between 19.8 nm $Si_{0.15}Ge_{0.85}$ barriers is grown on top.

The corresponding linear absorption spectrum is shown in Fig. 5(a). The typical steplike behavior and Coulomb enhancement are observed even at room temperature. The transitions are identified by a comparison to tight-binding calculations for a similar structure[17] and are in accordance with the findings in Ref. 18. The direct band gap at room temperature is found at 0.87 eV, corresponding to the transition from the first heavy-hole valence band hh1 to the first direct conduction band minimum cΓ1, labeled as hh1-cΓ1. Next, the light-hole-related transition lh1-cΓ1 is observed at 0.92 eV,

followed by the hh2-cΓ2 transition at 0.94 eV, and the lh2-cΓ2 transition at 0.99 eV. All electrons will eventually accumulate in the off-center states of the Brillouin zone due to the indirect nature of the conduction band.

The two false-color plots Figs. 5(b) and 5(c) show the differential absorption spectra at 293 K for two different injection energies with time delays between pump and probe varying from −200 to +600 fs as false-color plots, analogous to the discussion of the first sample. The black arrows indicate the dominant scattering processes acting as guide to the eye; the gray pulse shapes indicate the respective pump spectra.

Figure 5(b) shows the differential absorption for an injection of 1×10^{17} cm^{-2} at 1.02 eV high into the bands at the hh3-cΓ3 transition. A carrier distribution centered around the point of injection is observed shortly after excitation. Very few scattering processes have occurred and thus the carriers cannot yet be described by a Fermi distribution. Subsequently, the carriers undergo a cascaded relaxation over about 500 fs. The intermediate transitions at lower energies, lh2-cΓ2, hh2-cΓ2, and lh1-cΓ1, are successively bleached as the carriers relax toward the fundamental direct transition hh1-cΓ1. Scattering into higher states under phonon assistance and elastic scattering processes within the carrier system is only weakly observed. The overall amplitude of bleaching in the differential absorption signal decreases with increasing time delay. Simultaneously, a redshift of the hh1-cΓ1 transition is observed from time zero onwards, much earlier than the maximum bleaching of the hh1-cΓ1 transition, which occurs roughly 400 fs after the injection. This signature is caused by screening of electronic charges by free carriers. In general, free carriers lead to a renormalization of the band structure resulting in a shift of the resonances.[8] Since the shift of a resonance is not necessarily related to the population at the states involved in the transition, no scattering processes into these states need take place for the shift to occur. Similar to (GaIn)As, the shifts therefore set in quasi-instantaneously, i.e., after a delay which is below the temporal resolution of our experimental setup. Eventually, all electrons have scattered into the L valley after 500 fs. At that point, the system has reached a state of thermal quasiequilibrium with a long lifetime of considerably more than the 1 ns which is experimentally accessible in our setup. No change in the differential absorption is observed over this time span. Typically, high-quality samples of Ge exhibit lifetimes up to several μs.[19]

The scattering to higher energies is more pronounced for resonant optical pumping of the fundamental transition at an energy of 0.88 eV with a photon density of 3.5×10^{17} cm^{-2} as shown in Fig. 5(c). Scattering into states higher in energy, most notably at the hh2−cΓ2 transition, is observed for these excitation conditions. Here, the energy necessary for heating the carrier system is gained mainly from scattering to the indirect L valley: Electrons are transferred into the L valley by interaction with phonons. There, the electrons have larger excess energy with respect to the L minimum than they had with respect to the Γ minimum prior to scattering. They subsequently scatter downwards in energy by dissipating energy into the lattice via phonons, but also by interacting with electrons in the Γ valley, to which

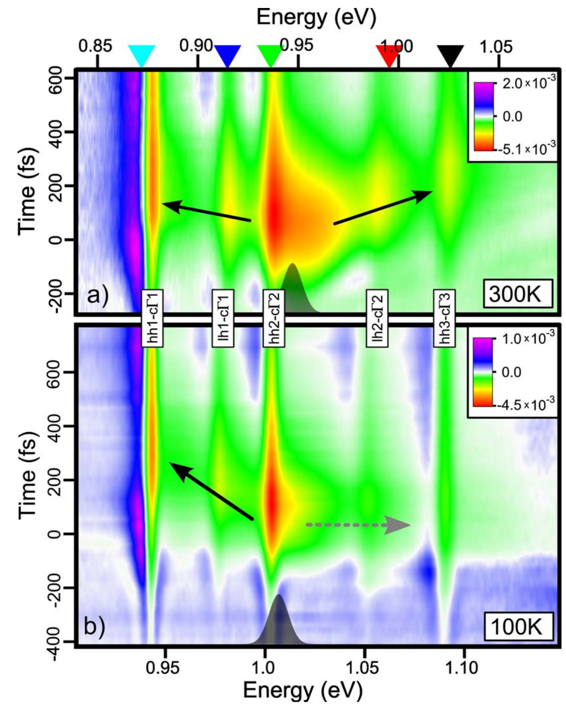

FIG. 6. (Color online) False-color-coded differential absorption spectra for (a) 293 and (b) 100 K lattice temperature. The sample is excited at the hh2-cΓ2 transition in both cases, as indicated by the gray pulse shape. The colored arrowheads at the top indicate the spectral positions of the time traces shown in Fig. 7.

they transfer the energy they gain in this process. The whole carrier system is considerably heated up by this process. An upper limit for the potential temperature increase ΔT is estimated taking into account the separation of Γ point and L point in energy of 136 meV, which corresponds to $\Delta T = 136\ \text{meV}/k_B \approx 1580$ K, where k_B is Boltzmann's constant. The actual temperature gain lies significantly below this number since phonon interaction quickly dissipates the energy into the lattice. Note that the mechanism described here does not specifically rely on off-center states such as L states. It is also effective in direct semiconductors as soon as carriers are injected with excess energy to the ground-state transition. However, in an indirect semiconductor the energy transfer is also possible for resonant excitation of the lowest direct transition, since carriers gain energy by scattering into the lower-lying off-center states. In the sample presented here, all electrons have scattered into the vicinity of the L minimum after about 200 fs.

Finally, the influence of the lattice temperature on the scattering dynamics is investigated in order to determine the role of phonon scattering. Differential absorption spectra for time delays between pump and probe of −200 to 600 fs are shown for lattice temperatures of 100 and 293 K in the top and bottom part Fig. 6, respectively. The carriers are in both cases injected close to the hh2-cΓ2 transition (gray pulse shape), again ensuring comparable excitation conditions, i.e., comparable magnitude of absorption and therefore comparable density of generated carriers. A photon flux of 1×10^{17} cm^{-2} is applied. Note that although this photon flux is more than two orders of magnitude higher than that used

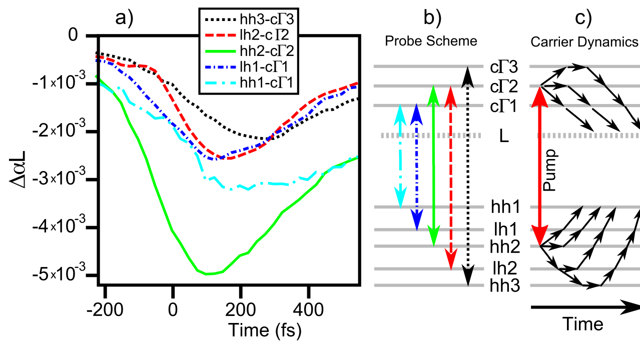

FIG. 7. (Color online) Temporal evolution of the differential absorption (a) at the transition energies as shown in the center part (b). The time traces reveal the scattering dynamics in the carrier system as schematically depicted in (c). Here, both scattering to states higher in energy is observed as well as depopulation of the cΓ states to the L valley.

for the (GaIn)As sample, the generated carrier densities are comparable. As shown in Refs. 8 and 20 by comparison with a microscopic theory, a photon flux of 1×10^{16} cm^{-2} yields a carrier density on the order of 1×10^{12} cm^{-2} in (GaIn)As, while in Ge a photon flux of 1×10^{18} cm^{-2} is required for the same carrier density. Pronounced scattering to higher and lower energies is found at room temperature as shown in Fig. 6(a). Shortly after excitation, carriers are transferred into states higher and lower in energy as indicated by the two black arrows on the left hand side of the figure. Thus, both scattering processes shown in Figs. 5(b) and 5(c) are observed simultaneously.

The relaxation is much slower when the sample is cooled to 100 K lattice temperature. The scattering times can now be extracted using the slopes of the differential absorption signal at the hh2-cΓ2 and hh1-cΓ1 transitions yielding 200 and 80 fs for 100 and 293 K, respectively. Also, note that, at 100 K, scattering to higher energies does not occur significantly. Only quasi-instantaneous redshifts are observed at resonances higher in energy than the point of injection, as can be seen by the neighboring bluish and greenish vertical lines at the respective transitions. Here, no population is created. Again, the shifts are caused by charge screening of carriers at lower energies which retroact on the band structure and not by population at the energies where the shift is actually observed.[8] At these temperatures, it is clear that the shifts are much faster than population transfer, as indicated by the dashed gray arrow. This clearly indicates that fast electron-electron interactions fuel the energy-conserving redistribution of charges which causes the screening, while the carrier cooling is mediated via phonons. As in the (GaIn)As sample, phonon absorption is distinctly reduced at low temperatures which results in a reduced efficiency of carrier cooling. This is directly observed in Figs. 6(a) and 6(b) when comparing the steepness of the black arrows which in each case demonstrate the carrier population transfer. Relaxation is thus slower under these conditions. In addition, scattering into states higher in energy is less pronounced here: fewer phonons are available to scatter electrons into the L valley and thereby, these fewer electrons provide less energy for electrons in the Γ valley to scatter to higher energies. Additional control experiments for much stronger and much weaker excitation (not shown here) yield no significant change in the scattering dynamics; i.e., any changes related to carrier density are much smaller than temperature-induced effects. In conclusion, strong Coulomb effects such as carrier-carrier scattering cause screening of charges but do not contribute to cooling, which confirms the role of phonons in thermalization.

The temporal dynamics at 300 K are analyzed further by investigating the time traces in Fig. 7(a) taken at the spectral positions indicated by the color coded arrows in Fig. 7(b), corresponding to the energies marked in Fig. 6(a). The maximum amplitude of the hh2-cΓ2 transition shown in green (solid) is populated directly after the excitation within 100 fs. No energy transfer is required here and the maximum bleaching is induced very quickly. The following decay is featureless until the quasisteady-state is reached after about 700 fs.

The carriers are scattered into states higher in energy by momentum transfer out of the unbalanced phonon bath and via elastic scattering processes inside the carrier system. The time traces of the lh2-cΓ2 and hh3-cΓ3 transition shown in red (dashed) and black (dotted) reach their extremes about 150 and 275 fs after excitation, respectively. This indicates a scattering time of $\tau_{\downarrow}=50$ fs to states involved in the transition lower in energy and $\tau_{\uparrow}=175$ fs to those higher in energy. The process of carrier redistribution is schematically depicted in Fig. 7(c).

The germanium material system displays slower dynamics than those found for (GaIn)As. The scattering of carriers toward the band edges after optical excitation with high excess energy takes about 200 fs for an excess energy of 100 meV in Ge, while in (GaIn)As 200 fs are determined for an excess energy of more than 200 meV. The compound semiconductor material (GaIn)As exhibits polar-optical scattering or Fröhlich interaction,[21,22] which is not present in elementary group IV semiconductors. Typical scattering times for optical phonon in III-V compound semiconductors are on the order of 100 fs (Refs. 23–26) but strongly depend on the respective ionic character of the material[27] and on the change in quasimomentum.[28] Deformation potential scattering of optical phonons is the dominant scattering process in case of silicon and germanium. It is rather inefficient for small momentum transfer but becomes very efficient for large momentum differences such as scattering from the Γ into the L valley.[28]

In conclusion, we investigated the carrier relaxation dynamics in (GaIn)As and Ge QWs as examples for III-V and group IV semiconductors, respectively. The samples were excited with varying excess energy above the band gap at ambient and at cryogenic temperatures. Pronounced scattering to energies above the point of carrier injection was observed in Ge for moderate excess energies. For high excess energy, nonthermal electron distributions form and the cooling process takes place on a time scale of several 100 fs. In this case, phonon-electron scattering was found to be more efficient than electron-electron scattering which gets less probable for the higher values of momentum transfer $\Delta\vec{k}$ (Ref. 13) which are required for thermalization here. In Ge, only deformation potential scattering contributes to cooling

due to the purely covalent nature of the Ge bonds. Contrarily, the compound material (GaIn)As has partly ionic bonds and the relaxation is thus slightly faster due to Fröhlich interaction.

The authors thank W. W. Rühle and S. W. Koch for helpful and constructive discussions and acknowledge financial support by the Deutsche Forschungsgemeinschaft, the Swiss Science Foundation, and the CARIPLO project MANDIS.

*christoph.lange@physik.uni-marburg.de

[1] H. Haug and S. W. Koch, *Quantum Theory of the Optical and Electronic Properties of Semiconductors*, 4th ed. (World Scientific, Singapore, 2004).
[2] H. J. Polland, W. W. Rühle, J. Kuhl, K. Ploog, K. Fujiwara, and T. Nakayama, Phys. Rev. B **35**, 8273 (1987).
[3] W. H. Knox, C. Hirlimann, D. A. B. Miller, J. Shah, D. S. Chemla, and C. V. Shank, Phys. Rev. Lett. **56**, 1191 (1986).
[4] J. L. Oudar, D. Hulin, A. Migus, A. Antonetti, and F. Alexandre, Phys. Rev. Lett. **55**, 2074 (1985).
[5] C. L. Petersen and S. A. Lyon, Phys. Rev. Lett. **65**, 760 (1990).
[6] T. Elsaesser, J. Shah, L. Rota, and P. Lugli, Phys. Rev. Lett. **66**, 1757 (1991).
[7] Y. Kuo, Y. Lee, Y. Ge, S. Ren, J. Roth, T. Kamins, D. Miller, and J. Harris, Nature (London) **437**, 1334 (2005).
[8] C. Lange, N. S. Köster, S. Chatterjee, H. Sigg, D. Chrastina, G. Isella, H. von Känel, M. Schäfer, M. Kira, and S. W. Koch, Phys. Rev. B **79**, 201306(R) (2009).
[9] J. Liu, X. Sun, L. Kimerling, and J. Michel, Opt. Lett. **34**, 1738 (2009).
[10] S. Koch, N. Peyghambarian, and M. Lindberg, J. Phys. C **21**, 5229 (1988).
[11] J. Shah, *Ultrafast Spectroscopy of Semiconductors and Semiconductor Nanostructures* (Springer, New York, 1996).
[12] C. Klingshirn, *Semiconductor Optics* (Springer-Verlag, Berlin, 2007).
[13] H. Haug and S. W. Koch, *Quantum Theory of the Optical and Electronic Properties of Semiconductors* (World Scientific, London, 2004).
[14] G. Sun, L. Friedman, and R. A. Soref, Phys. Rev. B **62**, 8114 (2000).
[15] M. Beye, F. Hennies, M. Deppe, E. Suljoti, M. Nagasono, W. Wurth, and A. Fohlisch, Phys. Rev. Lett. **103**, 237401 (2009).
[16] B. Rössner, D. Chrastina, G. Isella, and H. von Känel, Appl. Phys. Lett. **84**, 3058 (2004).
[17] M. Virgilio and G. Grosso, J. Phys.: Condens. Matter **18**, 1021 (2006).
[18] M. Bonfanti, E. Grilli, M. Guzzi, M. Virgilio, G. Grosso, D. Chrastina, G. Isella, H. von Känel, and A. Neels, Phys. Rev. B **78**, 041407(R) (2008).
[19] R. N. Hall, Phys. Rev. **87**, 387 (1952).
[20] C. Lange, S. Chatterjee, C. Schlichenmaier, A. Thränhardt, S. W. Koch, W. W. Rühle, J. Hader, J. V. Moloney, G. Khitrova, and H. M. Gibbs, Appl. Phys. Lett. **90**, 251102 (2007).
[21] H. Frohlich, Proc. R. Soc. London, Ser. A **215**, 291 (1952).
[22] R. Lassnig, Phys. Rev. B **30**, 7132 (1984).
[23] C. L. Collins and P. Y. Yu, Phys. Rev. B **30**, 4501 (1984).
[24] M. U. Wehner, M. H. Ulm, D. S. Chemla, and M. Wegener, Phys. Rev. Lett. **80**, 1992 (1998).
[25] W. A. Hügel, M. F. Heinrich, M. Wegener, Q. T. Vu, L. Bányai, and H. Haug, Phys. Rev. Lett. **83**, 3313 (1999).
[26] Q. T. Vu, H. Haug, W. A. Hügel, S. Chatterjee, and M. Wegener, Phys. Rev. Lett. **85**, 3508 (2000).
[27] K. T. Tsen, D. K. Ferry, A. Botchkarev, B. Sverdlov, A. Salvador, and H. Morkoç, Appl. Phys. Lett. **71**, 1852 (1997).
[28] P. Yu and M. Cardona, *Fundamentals of Semiconductors*, 2nd ed. (Springer, Berlin, 2003).